ELSEVIER

Journal of Organometallic Chemistry 658 (2002) 77–87

Journal of Organometallic Chemistry

www.elsevier.com/locate/jorganchem

3,3-Dimethyl-1-butyne complexes of tungsten(II). Crystal structures of [$WI_2(CO)(NCPh)(\eta^2\text{-}HC_2Bu^t)_2$] and [$WI_2(CO)\{P(OR)_3\}_2(\eta^2\text{-}HC_2Bu^t)$] (R = Me and Et)

Paul K. Baker [a,*], Michael G.B. Drew [b], Deborah S. Moore [a]

[a] *Department of Chemistry, University of Wales, Bangor, Gwynedd LL57 2UW, UK*
[b] *Department of Chemistry, University of Reading, Whiteknights, Reading RG6 6AD, UK*

Received 26 April 2002; received in revised form 25 May 2002; accepted 25 May 2002

Abstract

Reaction of [$WI_2(CO)_3(NCMe)_2$] with two equivalents of 3,3-dimethyl-1-butyne (HC_2Bu^t) in CH_2Cl_2 at room temperature, in the absence of light, afforded the bis(alkyne) complex, [$WI_2(CO)(NCMe)(\eta^2\text{-}HC_2Bu^t)_2$], **1**, in high yield. Nitrile exchange reactions of **1** with NCR (R = Et, Pr^i, Bu^t, Ph) gave the complexes [$WI_2(CO)(NCR)(\eta^2\text{-}HC_2Bu^t)_2$], (**2**–**5**). Complex **5** (R = Ph) was structurally characterised by a single crystal X-ray diffraction study and has a *pseudo*-octahedral geometry, with *cis* and parallel 3,3-dimethyl-1-butyne ligands, *trans* to the two mutually *cis*-iodo ligands, in the equatorial plane. The benzonitrile and carbon monoxide ligands are in the axial sites. The *tert*-butyl groups on the alkyne ligands are *trans* to one another. Treatment of **1** with two equivalents of $P(OR)_3$ in Et_2O afforded the bis(phosphite) complexes, [$WI_2(CO)\{P(OR)_3\}_2(\eta^2\text{-}HC_2Bu^t)$] {R = Me, **6**; Et **7**; Pr^i **8**}. The structures of **6** and **7** have been crystallographically determined with both complexes having similar *pseudo*-octahedral structures. The structures may be represented by two *cis* phosphite ligands in the equatorial plane with an iodo group and the carbonyl ligand, whilst the second iodo-group and the 3,3-dimethyl-1-butyne ligand are in the axial positions. Reaction of **6**–**8** with one equivalent of Ag[BF_4] in acetonitrile, in the absence of light, yielded the cationic complexes, [$WI(CO)(NCMe)\{P(OR)_3\}_2(\eta^2\text{-}HC_2Bu^t)$][$BF_4$] (**9**–**11**). Detailed ^1H, $^{13}C\{^1H\}$, ^{13}C–^1H and $^{31}P\{^1H\}$-NMR studies are described, which gave comprehensive structural information on these complexes in solution.

Keywords: 3,3-Dimethyl-1-butyne; Tungsten(II); Crystal structures; Carbonyl; Iodo

1. Introduction

Alkynes have played a prominent role in the history of organometallic chemistry. It is mainly during the past 30 years that the alkyne chemistry of molybdenum(II) and tungsten(II) has been investigated [1,2]. To date, the majority of the literature work on bis(alkyne) complexes of Mo(II) and W(II) containing halogens and/or carbonyl ligands has involved symmetrical alkynes such as 2-butyne [3–11], diphenylacetylene [3–5,7,8,11], hexafluoro-2-butyne [6,12,13], and 3-hexyne [7,14]. Complexes of the general type [$MXX'(CO)(NCMe)(\eta^2\text{-}RC_2R)_2$] [3,8,10,14] and [$\{M(\mu\text{-}X)X'(CO)(NCMe)(\eta^2\text{-}RC_2R)\}_2$] (X = Br or I) [8,10,11], have been well-established by Baker and co-workers.

Complexes containing unsymmetric alkynes, RC_2R', are less common; dimeric complexes, [$\{M(\mu\text{-}I)I(CO)(NCMe)(\eta^2\text{-}RC_2R')\}_2$], (M = Mo, W; R = Ph, R′ = Me, CH_2OH; R = Me, R′ = PhS, *p*-TolS) [11], [$\{W(\mu\text{-}I)Br(CO)(NCMe)(\eta^2\text{-}MeC_2Ph)\}_2$] [10], and [$WBr_2(CO)(\eta^2\text{-}MeC_2Ph)_2$] [15] and monomeric complexes such as [$WXX'(CO)(NCMe)(\eta^2\text{-}PhC_2Me)_2$] [8,10], [$Mo(CO)(\eta^2\text{-}RC_2R')_2(\eta^5\text{-}C_5H_5$ or $C_9H_7)$][BF_4] (R = H, R′ = Me; R = H, R′ = Bu^t; R = Me, R′ = Ph) [4] and [$Mo(NCMe)(\eta^2\text{-}RC_2R')_2(\eta^5\text{-}C_5H_5$ or $C_9H_7)$][BF_4] (R = R′ = Me; R = H, R′ = Bu^t; R = H, R′ = Pr^i, R = Me, R′ = Ph) [5], have been reported.

In this paper, we describe the synthesis of a series of 3,3-dimethyl-1-butyne complexes of tungsten(II) of the type [$WI_2(CO)(NCR)(\eta^2\text{-}HC_2Bu^t)_2$] {R = Me, Et, Pr^i, Bu^t, Ph (crystallographically characterised)}(**1**–**5**),

---

* Corresponding author. Fax: +44-1248-370528
E-mail address: chs018@bangor.ac.uk (P.K. Baker).

0022-328X/02/$ - see front matter © 2002 Elsevier Science B.V. All rights reserved.
PII: S0022-328X(02)01630-3

$[WI_2(CO)\{P(OR)_3\}_2(\eta^2\text{-}HC_2Bu^t)]$ {R = Me, Et, (both crystallographically characterised), Pr^i}(**6**–**8**) and $[WI(CO)(NCMe)\{P(OR)_3\}_2(\eta^2\text{-}HC_2Bu^t)][BF_4]$ {R = Me, Et, Pr^i}(**9**–**11**). Detailed NMR studies were carried out to give structural information about many of these complexes in solution.

2. Results and discussion

2.1. *Synthesis and NMR studies of $[WI_2(CO)(NCMe)(\eta^2\text{-}HC_2Bu^t)_2]$ (**1**)*

Two equivalents of 3,3-dimethyl-1-butyne were added to a solution of $[WI_2(CO)_3(NCMe)_2]$ [16] in dichloromethane, in a foil-covered Schlenk tube, and the solution stirred for 22 h. Filtration over celite, removal of the solvent in vacuo, followed by recrystallisation from diethyl ether–hexane solution (8 cm^3, 1:1) cooled to −17 °C, gave single dark yellow crystals of $[WI_2(CO)(NCMe)(\eta^2\text{-}HC_2Bu^t)_2]$ **1** which were unsuitable for X-ray crystallography. Complex **1** was fully characterised by elemental analysis (C, H, N), IR spectroscopy, ^1H-NMR spectroscopy and $^{13}C\{^1H\}$-NMR spectroscopy (Tables 1–4). It is very soluble in acetonitrile, diethyl ether, chlorinated solvents and hydrocarbon solvents such as hexane. The solid complex is stable in air for up to 15 min and can be kept under nitrogen at −17 °C for up to 2 months, with no apparent decomposition. In solution, however, the complex is less stable and decomposes within 24 h upon exposure to air.

The IR spectrum of **1** (Table 2), shows a strong carbonyl band at 2074 cm^{-1}, a weak asymmetric doublet due to the acetonitrile at 2324 and 2297 cm^{-1}, and two weak alkyne stretching bands at 1710 and 1691 cm^{-1}. The $\nu(C\equiv C)$ stretching band for the coordinated alkyne was found at a lower wavenumber than for uncoordinated unsymmetric alkynes (2260–2190 cm^{-1}) [17], due to synergic bonding between the tungsten metal and the alkyne ligands.

Table 2
Infrared data [a] for the HC_2Bu^t complexes **1**–**11**

Complex	$\nu(C\equiv N)$ (cm^{-1})	$\nu(C\equiv O)$ (cm^{-1})	$\nu(C\equiv C)$ (cm^{-1})
1	2324, 2297, w	2074, s, sh	1710, 1691, w
2	2295, w	2074, s, sh	1710, 1692, w
3	2292, m	2072, s, sh	1710, 1692, w
4	2286, w	2074, s, sh	1710, 1692, w
5	2274, m	2077, s, sh	1709, 1690, w
6		1999, s	1654, w
7		1992, s	1654, w
8		1981, s	1655, w
9	2292, w	1985, s, br	1653, w
10	2322, 2293, w	1978, s, br	1624, w
11	2292, w	1976, s, br	1624, w

s, Strong; m, medium; w, weak; sh, sharp.
[a] Spectra recorded as thin films in $CHCl_3$, between NaCl plates.

The ^1H-NMR spectrum of complex **1** (Table 3), showed two singlets at $\delta = 10.95$ and 10.15 ppm, (2 × 1H, $\mathbf{H}C_2Bu^t$), acetonitrile methyl protons at 2.84 ppm and the methyl protons of the *tert*-butyl groups as two overlapping singlets at 1.39 ppm (9H, $HC_2\mathbf{Bu^t}$) and 1.38 ppm (9H, HC_2Bu^t). The terminal hydrogens of alkynes, are usually detected at low chemical shifts when the alkyne is coordinated to a transition metal centre; Tatsumi and co-workers [18], reported acetylene and phenylacetylene signals at 10.43 and 10.40 ppm for complexes of the type $[Mo(SBu^t)_2(CNBu^t)_2(\eta^2\text{-}RC_2R')]$, (R = R′ = H and R = H, R′ = Ph). Ward and Templeton [19] suggested that four-electron donor alkynes have lower field resonances (around 12 ppm) than those observed for two-electron donor alkynes (around 7 or 8 ppm), which would indicate that the observed values for the terminal protons of **1** are characteristic of three-electron donor alkynes, (i.e. between the values for two- and four-electron donors),

Table 1
Physical and analytical data [a] for the HC_2Bu^t complexes **1**–**11**

	Complex	Colour	Yield %	Analysis (%)		
				C	H	N
1	$[WI_2(CO)(NCMe)(\eta^2\text{-}HC_2Bu^t)_2]$	Gold–brown	88	27.0 (26.8)	3.4 (3.5)	1.7 (2.1)
2	$[WI_2(CO)(NCEt)(\eta^2\text{-}HC_2Bu^t)_2]$	Green–yellow	56	28.2 (28.1)	3.5 (3.7)	1.6 (2.0)
3	$[WI_2(CO)(NCPr^i)(\eta^2\text{-}HC_2Bu^t)_2]$	Green–yellow	87	29.7 (29.2)	3.9 (3.9)	1.8 (2.0)
4	$[WI_2(CO)(NCBu^t)(\eta^2\text{-}HC_2Bu^t)_2]$	Green–yellow	78	30.6 (30.3)	4.1 (4.1)	1.8 (2.0)
5	$[WI_2(CO)(NCPh)(\eta^2\text{-}HC_2Bu^t)_2]$	Green–yellow	77	32.6 (32.7)	3.4 (3.4)	1.9 (1.9)
6	$[WI_2(CO)\{P(OMe)_3\}_2(\eta^2\text{-}HC_2Bu^t)]$	Dark green	70	19.6 (19.6)	3.4 (3.5)	
7	$[WI_2(CO)\{P(OEt)_3\}_2(\eta^2\text{-}HC_2Bu^t)]$	Dark green	90	26.3 (25.9)	4.4 (4.6)	
8	$[WI_2(CO)\{P(OPr^i)_3\}_2(\eta^2\text{-}HC_2Bu^t)]$	Dark green	88	31.9 (31.1)	5.4 (5.4)	
9	$[WI(CO)(NCMe)\{P(OMe)_3\}_2(\eta^2\text{-}HC_2Bu^t)][BF_4]$	Red–brown	62	23.0 (22.6)	4.3 (3.9)	1.1 (1.8)
10	$[WI(CO)(NCMe)\{P(OEt)_3\}_2(\eta^2\text{-}HC_2Bu^t)][BF_4]$	Red–brown	63	29.4 (28.6)	5.1 (4.9)	1.1 (1.6)
11	$[WI(CO)(NCMe)\{P(OPr^i)_3\}_2(\eta^2\text{-}HC_2Bu^t)][BF_4]$	Red–brown	66	33.8 (33.6)	5.4 (5.7)	1.1 (1.5)

[a] Calculated values in parentheses.

Table 3
Proton NMR data [a] for the $\mathrm{HC_2Bu}^t$ complexes **1**–**11**

	^{1}H (δ) ppm
1	10.95 (s, 1H, $\mathbf{HC}_2\mathrm{Bu}^t$); 10.15 (s, 1H, $\mathbf{HC}_2\mathrm{Bu}^t$); 2.84 (s, 3H, $\mathbf{CH}_3\mathrm{CN}$); 1.39 (s, 9H, $\mathrm{HC_2C}(\mathbf{CH}_3)_3$), 1.38 (s, 9H, $\mathrm{HC_2C}(\mathbf{CH}_3)_3$)
2	10.83 (s, 1H, $\mathbf{HC}_2\mathrm{Bu}^t$); 10.01 (s, 1H, $\mathbf{HC}_2\mathrm{Bu}^t$); 3.13 (q, 2H, $\mathrm{CH_3}\mathbf{CH}_2\mathrm{CN}$, $J = 7.6$ Hz, 15.2 Hz); 1.65 (t, 3H, $\mathbf{CH}_3\mathrm{CH_2CN}$, $J = 7.6$ Hz); 1.39 (s, 18H, $\mathrm{HC_2C}(\mathbf{CH}_3)_3$)
3	10.82 (s, 1H, $\mathbf{HC}_2\mathrm{Bu}^t$); 9.99 (s, 1H, $\mathbf{HC}_2\mathrm{Bu}^t$); 3.51–3.40 (m, 1H, $\mathrm{(CH_3)_2}\mathbf{CH}\mathrm{CN}$); 1.66 (d, 6H, $(\mathbf{CH}_3)_2\mathrm{CHCN}$, $J = 7.1$ Hz); 1.39 (s, 18H, $\mathrm{HC_2C}(\mathbf{CH}_3)_3$)
4	10.81 (s, 1H, $\mathbf{HC}_2\mathrm{Bu}^t$); 9.99 (s, 1H, $\mathbf{HC}_2\mathrm{Bu}^t$); 1.69 (s, 9H, $(\mathbf{CH}_3)_3\mathrm{CCN}$); 1.42 (s, 18H, $\mathrm{HC_2C}(\mathbf{CH}_3)_3$)
5	10.85 (s, 1H, $\mathbf{HC}_2\mathrm{Bu}^t$); 10.15 (s, 1H,$\mathbf{HC}_2\mathrm{Bu}^t$); 8.10–7.40 (m, 5H, $\mathbf{Ph}\mathrm{CN}$); 1.44 (s, 9H, $\mathrm{HC_2C}(\mathbf{CH}_3)_3$); 1.42 (s, 9H, $\mathrm{HC_2C}(\mathbf{CH}_3)_3$)
6	12.28 (dd, 1H, $\mathbf{HC}_2\mathrm{C(CH_3)_3}$, $J = 2.5$ Hz, $J_{\mathrm{P-H}} = 25.3$ Hz); 3.88 (d, 9H, $\mathrm{OC}\mathbf{H}_3$, $J_{\mathrm{P-H}} = 10.0$ Hz); 3.43 (d, 9H, $\mathrm{OC}\mathbf{H}_3$, $J_{\mathrm{P-H}} = 10.8$ Hz); 1.44 (s, 9H, $\mathrm{HC_2C}(\mathbf{CH}_3)_3$)
7	12.11 (dd, 1H, $\mathbf{HC}_2\mathrm{C(CH_3)_3}$, $J = 2.5$ Hz, $J_{\mathrm{P-H}} = 25.0$ Hz); 4.16–4.10 (m, 6H, $\mathrm{OC}\mathbf{H}_2\mathrm{CH_3}$); 3.80–3.73 (m, 6H, $\mathrm{OCH_2C}\mathbf{H}_3$); 1.43 (s, 9H, $\mathrm{HC_2C}(\mathbf{CH}_3)_3$); 1.31 (t, 9H, $\mathrm{OC}\mathbf{H}_2\mathrm{CH}_{3,}$ $J = 7.0$ Hz); 1.10 (t, 9H, $\mathrm{OCH_2C}\mathbf{H}_3$, $J = 7.0$ Hz)
8	13.36 (s, 1H, $\mathbf{HC}_2\mathrm{C(CH_3)_3}$); 11.96 (dd, 1H, $\mathbf{HC}_2\mathrm{C(CH_3)_3}$, $J = 2.9$ Hz, $J_{\mathrm{P-H}} = 25.4$ Hz); 4.90–4.65 (m, 6H, $\mathrm{(CH_3)_2C}\mathbf{HO}$)-*trans*; 4.55–4.45 (m, 6H, $\mathrm{(CH_3)_2C}\mathbf{HO}$)-*cis*; 1.90–1.10 (br m, 90H, $\mathrm{HC_2C}(\mathbf{CH}_3)_3$ (*cis* and *trans*), $(\mathbf{CH}_3)_2\mathrm{CHO}$ (*cis* and *trans*)
9	13.95 (s, 1H, $\mathbf{HC}_2\mathrm{C(CH_3)_3}$); 3.60–3.50 (m, 18H, $\mathrm{OC}\mathbf{H}_3$); 2.90 (s, 3H, $\mathbf{CH}_3\mathrm{CN}$); 1.60–1.40 (m, 9H, $\mathrm{HC_2C}(\mathbf{CH}_3)_3$)
10	13.70 (s, 1H, $\mathbf{HC}_2\mathrm{C(CH_3)_3}$); 3.95–3.70 (m, 12H, $\mathrm{OC}\mathbf{H}_2\mathrm{CH_3}$); 2.80 (s, 3H, $\mathbf{CH}_3\mathrm{CN}$); 1.45–1.05 (br m, 27H, $\mathrm{OCH_2C}\mathbf{H}_3$, $\mathrm{HC_2C}(\mathbf{CH}_3)_3$)
11	13.55 (s, 1H, $\mathbf{HC}_2\mathrm{C(CH_3)_3}$); 4.70–4.40 (m, 6H, $\mathrm{(CH_3)_2C}\mathbf{HO}$); 2.80 (s, 3H, $\mathbf{CH}_3\mathrm{CN}$); 1.50 (s, 9H, $\mathrm{HC_2C}(\mathbf{CH}_3)_3$); 1.30–1.05 (m, 36H, $(\mathbf{CH}_3)_2\mathrm{CHO}$)

s, Singlet; d, doublet; t, triplet; q, quartet; m, multiplet; br, broad.

[a] Spectra recorded in $\mathrm{CDCl_3}$ at +25 °C, referenced to $\mathrm{SiMe_4}$.

Table 4
Carbon NMR data [a] for the $\mathrm{HC_2Bu}^t$ complexes **1**–**7**

	^{13}C{^{1}H} (δ) ppm
1	205.24 (s, $\mathbf{C}\equiv\mathrm{O}$); 189.12 (s, $\mathrm{HC}\equiv\mathbf{C}\mathrm{Bu}^t$); 177.64 (s, $\mathrm{HC}\equiv\mathbf{C}\mathrm{Bu}^t$); 157.40 (s, $\mathrm{H}\mathbf{C}\equiv\mathrm{CBu}^t$); 149.36 (s, $\mathrm{H}\mathbf{C}\equiv\mathrm{CBu}^t$); 139.82 (s, $\mathrm{CH_3}\mathbf{C}\mathrm{N}$); 40.05 (s, $\mathrm{(CH_3)_3}\mathbf{C}$); 39.29 (s, $\mathrm{(CH_3)_3}\mathbf{C}$); 30.19 (m, 2 × $\mathrm{HC_2C}(\mathbf{CH}_3)_3$); 5.46 (s, $\mathbf{CH}_3\mathrm{CN}$)
2	205.10 (s, $\mathbf{C}\equiv\mathrm{O}$); 188.96 (s, $\mathrm{HC}\equiv\mathbf{C}\mathrm{Bu}^t$); 177.70 (s, $\mathrm{HC}\equiv\mathbf{C}\mathrm{Bu}^t$); 157.31 (s, $\mathrm{H}\mathbf{C}{=}\mathrm{CBu}^t$); 149.18 (s, $\mathrm{H}\mathbf{C}\equiv\mathrm{CBu}^t$); 139.69 (s, $\mathrm{CH_3CH_2}\mathbf{C}\mathrm{N}$); 40.01 (s, $\mathrm{(CH_3)_3}\mathbf{C}$); 39.34 (s, $\mathrm{(CH_3)_3}\mathbf{C}$); 30.15–29.27 (m, 2 × $\mathrm{HC_2C}(\mathbf{CH}_3)_3$); 13.31 (s, $\mathrm{CH_3}\mathbf{CH}_2\mathrm{CN}$); 9.21 (s, $\mathbf{CH}_3\mathrm{CH_2CN}$)
3	205.27 (s, $\mathbf{C}\equiv\mathrm{O}$); 188.95 (s, $\mathrm{HC}\equiv\mathbf{C}\mathrm{Bu}^t$); 177.65 (s, $\mathrm{HC}\equiv\mathbf{C}\mathrm{Bu}^t$); 157.45 (s, $\mathrm{H}\mathbf{C}\equiv\mathrm{CBu}^t$); 149.05 (s, $\mathrm{H}\mathbf{C}\equiv\mathrm{CBu}^t$); 139.74 (s, $\mathrm{(CH_3)_2CH}\mathbf{C}\mathrm{N}$); 39.99 (s, $\mathrm{(CH_3)_3}\mathbf{C}$); 39.37 (s, $\mathrm{(CH_3)_3}\mathbf{C}$); 30.15–29.29 (m, 2 × $\mathrm{HC_2C}(\mathbf{CH}_3)_3$); 19.92 (s, $\mathrm{(CH_3)_2}\mathbf{CH}\mathrm{CN}$); 18.74 (s, $(\mathbf{CH}_3)_2\mathrm{CHCN}$)
4	205.25 (s, $\mathbf{C}\equiv\mathrm{O}$); 188.79 (s, $\mathrm{HC}\equiv\mathbf{C}\mathrm{Bu}^t$); 177.69 (s, $\mathrm{HC}\equiv\mathbf{C}\mathrm{Bu}^t$); 157.51 (s, $\mathrm{H}\mathbf{C}\equiv\mathrm{CBu}^t$); 148.87 (s, $\mathrm{H}\mathbf{C}\equiv\mathrm{CBu}^t$); 139.72 (s, $\mathrm{(CH_3)_3}\mathbf{C}\mathrm{CN}$); 39.98 (s, $\mathrm{(CH_3)_3}\mathbf{C}$); 39.33 (s, $\mathrm{(CH_3)_3}\mathbf{C}$); 30.16–29.29 (m, 2 × $\mathrm{HC_2C}(\mathbf{CH}_3)_3$); 27.25 (s, $(\mathbf{CH}_3)_3\mathrm{CCN}$)
5	205.03 (s, $\mathbf{C}\equiv\mathrm{O}$); 188.56 (s, $\mathrm{HC}\equiv\mathbf{C}\mathrm{Bu}^t$); 177.72 (s, $\mathrm{HC}\equiv\mathbf{C}\mathrm{Bu}^t$); 157.26 (s, $\mathrm{H}\mathbf{C}\equiv\mathrm{CBu}^t$); 148.82 (s, $\mathrm{H}\mathbf{C}\equiv\mathrm{CBu}^t$); 139.73 (s, $\mathrm{Ph}\mathbf{C}\mathrm{N}$); 135.42–129.78 (m, $\mathbf{Ph}\mathrm{CN}$); 40.08 (s, $\mathrm{(CH_3)_3}\mathbf{C}$); 39.41 (s, $\mathrm{(CH_3)_3}\mathbf{C}$); 29.94 (s, $\mathrm{HC_2C}(\mathbf{CH}_3)_3$); 29.34 (s, $\mathrm{HC_2C}(\mathbf{CH}_3)_3$)
6	221.67 (s, $\mathbf{C}\equiv\mathrm{O}$); 213.09 (dd, $\mathrm{HC{-}}\mathbf{C}\mathrm{C(CH_3)_3}$, $J = 8.7$ Hz, $J_{\mathrm{P-C}} = 66.6$ Hz); 190.60 (dd, $\mathrm{H}\mathbf{C}\equiv\mathrm{CC(CH_3)_3}$, $J = 8.7$ Hz, $J_{\mathrm{P-C}} = 35.8$ Hz); 54.10 (dd, 2 × $\mathrm{PO}\mathbf{C}\mathrm{H_3)_3}$, $J = 7.6$ Hz, $J_{\mathrm{P-C}} = 36.9$ Hz); 41.69 (s, $\mathrm{HC\equiv C}\mathbf{C}\mathrm{(CH_3)_3}$); 30.19 (s, $\mathrm{HC\equiv CC}(\mathbf{C}\mathrm{H_3})_3$)
7	221.80 (t, $\mathbf{C}\equiv\mathrm{O}$, $J_{\mathrm{P-C}} = 6.2$ Hz); 213.74 (dd, $\mathrm{HC}\equiv\mathbf{C}\mathrm{C(CH_3)_3}$, $J = 8.3$ Hz, $J_{\mathrm{P-C}} = 66.0$ Hz); 191.25 (dd, $\mathrm{H}\mathbf{C}\equiv\mathrm{CC(CH_3)_3}$, $J = 8.3$ Hz, $J_{\mathrm{P-C}} = 35.9$ Hz); 62.68–62.30 (m, $\mathrm{P(O}\mathbf{C}\mathrm{H_2CH_3)_3}$); 41.51 (s, $\mathrm{HC\equiv C}\mathbf{C}\mathrm{(CH_3)_3}$); 30.21 (s, $\mathrm{HC\equiv CC}(\mathbf{C}\mathrm{H_3})_3$); 16.19–15.80 (m, $\mathrm{P(OCH_2}\mathbf{C}\mathrm{H_3)_3}$)

s, Singlet; d, doublet; m, multiplet; dd, double of doublet.

[a] Spectra recorded in $\mathrm{CDCl_3}$ at +25 °C, referenced to $\mathrm{SiMe_4}$.

which is substantiated by the ^{13}C{^{1}H}-NMR data for complex **1**.

In the ^{13}C{^{1}H}-NMR spectrum of complex **1** (Fig. 1(a)), the carbonyl resonance was observed at 205.24 ppm, and the alkyne contact carbon resonances at 189.12 and 177.64 ppm for $\mathrm{HC}\equiv\mathbf{C}\mathrm{Bu}^t$, and at 157.40 and 149.36 ppm for $\mathrm{H}\mathbf{C}\equiv\mathrm{CBu}^t$, respectively. The acetonitrile ($\mathrm{CH_3}\mathbf{C}\equiv\mathrm{N}$) resonance was observed at 139.82 ppm and the signal for the methyl group of the acetonitrile ($\mathbf{C}\mathrm{H_3C}\equiv\mathrm{N}$) at 5.46 ppm. Two *tert*-butyl signals were observed at 40.05 and 39.29 ppm which, coupled with the two distinct terminal hydrogen resonances in the proton NMR spectrum, confirm the presence of the *trans*-isomer only. This is also in good agreement with the solid state structure of $[\mathrm{WI_2(CO)(NCPh)}(\eta^2\text{-}\mathrm{HC_2Bu}^t)_2]$ **5** (Fig. 2), described in the next section.

A proton coupled ^{13}C-NMR spectrum of **1** was used to differentiate between the *tert*-butyl substituted alkyne carbon and the alkyne carbon with the hydrogen substituent, by comparison with the proton decoupled spectrum. In the coupled spectrum, Fig. 1(b), the singlet resonances at 157.40 and 149.36 ppm were split into doublets, which was indicative of one proton adjacent to each carbon and so were assigned to $\mathrm{H}\mathbf{C}\equiv\mathrm{CBu}^t$. From Templeton and Ward's correlation [20], the two alkynes donate an average of three electrons each to the tungsten centre.

2.2. *Preparation and characterisation of the nitrile exchanged complexes, $[\mathrm{WI_2(CO)(NCR)}(\eta^2\text{-}\mathrm{HC_2Bu}^t)_2]$ (2–5) (R = Et, Pr^i, Bu^t and Ph)*

The complexes **2**–**5**, $[\mathrm{WI_2(CO)(NCR)}(\eta^2\text{-}\mathrm{HC_2Bu}^t)_2]$ (R = Et, Pr^i, Bu^t and Ph) (**2**–**5**), were prepared by the reaction of **1** with one equivalent of NCR (R = Et, Pr^i, Bu^t, Ph) in dichloromethane for 22 h. All four complexes showed complete exchange of the acetonitrile group with the incoming nitrile ligand. The complexes **2**–**5** were all fully characterised by elemental analysis (C, H, N), IR spectroscopy, ^{1}H-NMR spectroscopy and ^{13}C{^{1}H}-NMR spectroscopy (Tables 1–4). They were all soluble in acetonitrile, diethyl ether and chlorinated solvents such as chloroform and dichloromethane, and partially soluble in hydrocarbon solvents such as hexane. The four complexes were stable in air for up

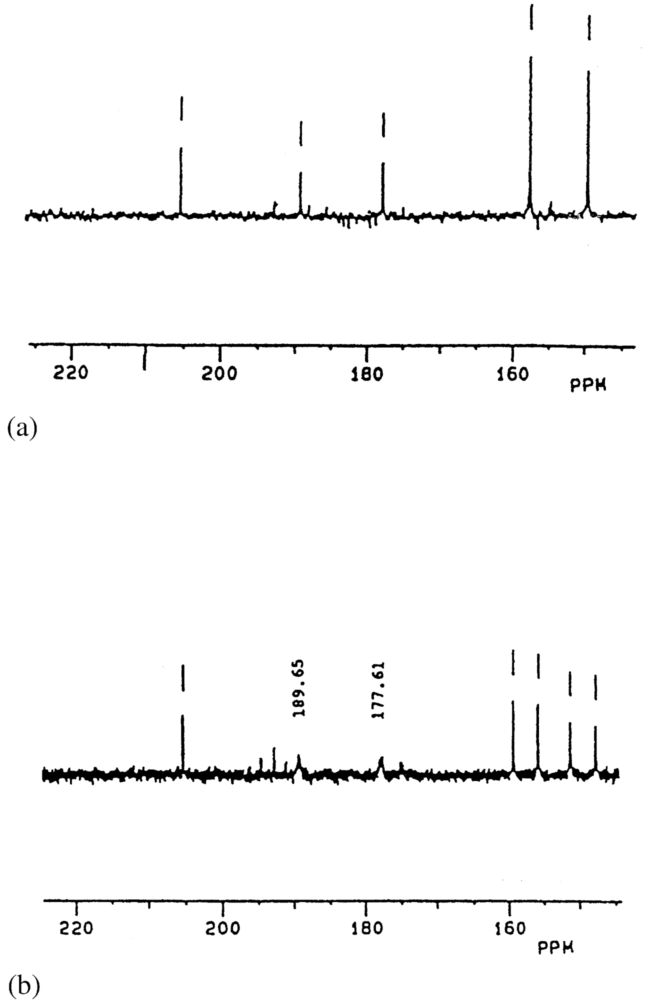

Fig. 1. The alkyne (C≡C) contact carbon region for (a) the $^{13}C\{^1H\}$-NMR spectrum and (b) the ^{13}C–^1H-NMR spectrum of $[WI_2(CO)(NCMe)(\eta^2\text{-}HC_2Bu^t)_2]$, **1**, ($CDCl_3$, 25 °C, referenced to $SiMe_4$).

to 10 min and were kept for 1 month at −17 °C, under nitrogen, with no obvious deterioration. Solutions of **2**–**5** were more sensitive, decomposing within 24 h at room temperature, when exposed to air, but could be kept under nitrogen at −17 °C for several weeks with no signs of decomposition.

The IR spectra of **2**–**5**, (Table 2), all show strong carbonyl stretching bands between 2077 and 2072 cm^{-1}, and two weak alkyne (C≡C) stretching bands, one at either 1710 or 1709 cm^{-1} and the other between 1692 and 1690 cm^{-1}. A weak nitrile stretching band between 2295 and 2274 cm^{-1} was observed for each complex, and there was a trend in the decrease in wavenumber of the nitrile peak with increase in size and chain length of the R group of R–C≡N. Complexes **2**–**5** are all similar in colour (green–yellow), and the detected carbonyl ν(C≡O) stretches and alkyne ν(C≡C) bands are similar, which seems to indicate that the R substituent of the nitrile ligand does not have a substantial effect on the electron donating or accepting properties of the nitrile ligands.

For all four complexes **2**–**5**, the ^1H-NMR spectra (Table 3) showed two terminal hydrogen resonances between 10.95 and 9.99 ppm, which indicated that the complexes had formed the *trans* isomer, exclusively. Complex **5** also had two distinct singlets at 1.44 and 1.42 ppm which were attributed to the methyl protons of the *tert*-butyl groups, thus supporting the formation of the *trans*-isomer.

The $^{13}C\{^1H\}$-NMR spectra of complexes **2**–**5** (Table 4), were also assigned for the *trans* isomer only, as described for complex **1**, but with the presence of signals associated with each of the nitrile ligands. As for **1**, complexes **2**–**5** had four alkyne contact carbon resonances and two quaternary *tert*-butyl carbon signals, which support the exclusive formation of the *trans*-isomers in solution. The chemical shifts of the alkyne carbons, between 188.96 and 148.82 ppm, indicate that the two alkynes are donating an average of three electrons each to the tungsten centre in these complexes [20].

Suitable single crystals of complex **5** were obtained for X-ray crystallography from a concentrated diethyl ether solution (6 cm^3), cooled to −17 °C for 20 h. The molecular structure is shown in Fig. 2, together with the atomic numbering scheme. Crystal data are given in Table 5 and selected bond lengths and angles are given in Table 6. The structure shows the *trans*-isomer with the two *tert*-butyl alkyne substituents on opposite sides, and it is apparent that the observed isomer is favoured on steric grounds, with the two Bu^t groups placed as far from one another as possible to minimise steric hindrance within the complex. The similarities in spectroscopic data for complexes **1**–**4** suggests that the four complexes probably have similar solid state structures to that of **5**.

Complexes $[WI_2(CO)(NCPh)(\eta^2\text{-}MeC_2Ph)_2]$ [21] and **5** are the first crystallographically characterised examples of *trans*-$[WI_2(CO)(NCR)(\eta^2\text{-}R'C_2R'')_2]$ (where R, R′ and R″ = alkyl or aryl, R′ ≠ R″). As for $[WI_2(CO)(NCPh)(\eta^2\text{-}MeC_2Ph)_2]$ [21], complex **5** is formally eight-coordinate, but by considering each alkyne as occupying one coordination site, it can be regarded as six-coordinate. In both $[WI_2(CO)(NCPh)(\eta^2\text{-}MeC_2Ph)_2]$ [21] and **5**, the carbonyl ligand was found to be *trans* to the benzonitrile group, with the two alkyne moieties mutually *cis*, and each alkyne *trans* to one iodine atom, as observed for complexes $[WI_2(CO)(NCR)(\eta^2\text{-}MeC_2Ph)_2]$ (R = Me, Et) [21] and $[WI_2(CO)(NCMe)(\eta^2\text{-}RC_2R)_2]$ (R = Me, Ph) [8].

The major difference between $[WI_2(CO)(NCR)(\eta^2\text{-}MeC_2Ph)_2]$ (R = Me, Et) [21], $[WI_2(CO)(NCPh)(\eta^2\text{-}MeC_2Ph)_2]$ [21] and **5** is the position of the alkyne substituents; in $[WI_2(CO)(NCR)(\eta^2\text{-}MeC_2Ph)_2]$ (R = Me, Et) [21], the two phenyl groups of 1-phenyl-1-

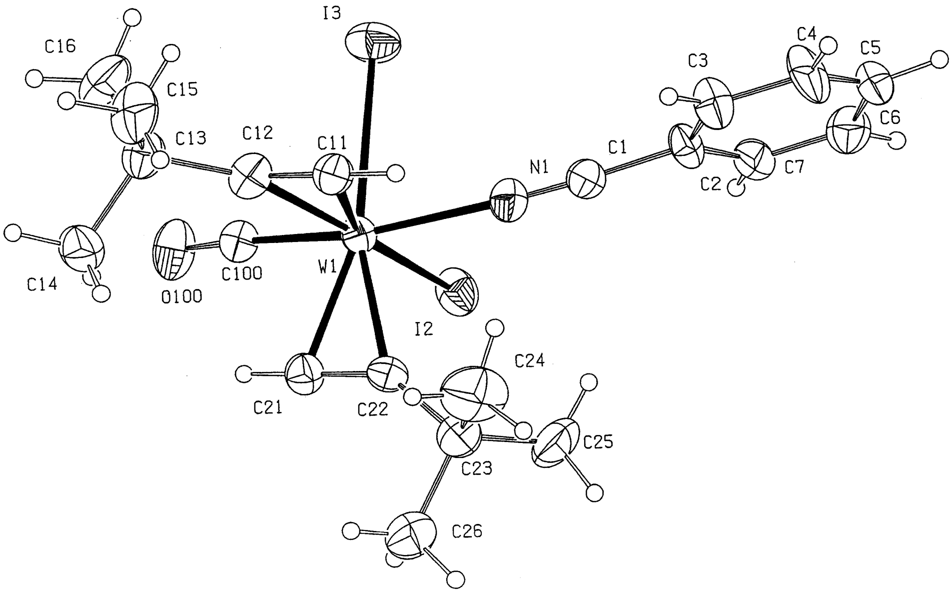

Fig. 2. Crystal structure of $[WI_2(CO)(NCPh)(\eta^2\text{-}HC_2Bu^t)_2]$ **5**, together with the atomic numbering scheme; ellipsoids shown at 30% probability.

propyne are opposite to one another (*cis*-isomer), whereas for $[WI_2(CO)(NCPh)(\eta^2\text{-}MeC_2Ph)_2]$ [21], and for **5**, the phenyl and methyl groups or the hydrogen and *tert*-butyl groups, respectively, are opposite to one another (*trans*-isomer).

The crystal structure of the related bis(2-butyne) complex, $[WI_2(CO)(NCPh)(\eta^2\text{-}MeC_2Me)_2]$ has been reported by Baker and co-workers [22]. The W–I bond lengths for $[WI_2(CO)(NCPh)(\eta^2\text{-}MeC_2Ph)_2]$, [2.872(3) and 2.909(3) Å] and **5** [2.883(3) and 2.897(3) Å] are comparable with those of $[WI_2(CO)(NCPh)(\eta^2\text{-}MeC_2Me)_2]$ [22], [2.8613(13) and 2.8407(13) Å], and the internal angles, I(2)–W(1)–I(3) of 83.30(8) and 82.34(5)° are similar to that of $[WI_2(CO)(NCPh)(\eta^2\text{-}MeC_2Me)_2]$ [22] at 83.53(4)°. The W–N bond lengths for $[WI_2(CO)(NCPh)(\eta^2\text{-}MeC_2Ph)_2]$ [21] and **5**, [2.171(14) and 2.167(10) Å, respectively]. These similarities suggest that the different alkynes do not overly affect the other tungsten–ligand bonds within the complexes $[WI_2(CO)(NCPh)(\eta^2\text{-}MeC_2Ph)_2]$ [21], **5** and $[WI_2(CO)(NCPh)(\eta^2\text{-}MeC_2Me)_2]$ [22].

The tungsten–carbon(carbonyl) bond lengths for $[WI_2(CO)(NCPh)(\eta^2\text{-}MeC_2Ph)_2]$ [21] and **5**, [2.054(16) and 2.037(12) Å, respectively], show that the two *trans*-isomers are similar to one another and they compare well with analogous bond lengths for the complexes

Table 5
Crystal data for the HC_2Bu^t complexes **5**–**7**

	5	**6**	**7**
Empirical formula	$C_{22}H_{21}I_2NOW$	$C_{13}H_{28}I_2O_7P_2W$	$C_{19}H_{40}I_2O_7P_2W$
Formula weight	733.05	795.94	880.10
Crystal system	Monoclinic	Monoclinic	Monoclinic
Space group	$P2_1/c$	$P2_1/n$	$P2_1/c$
Unit cell dimensions			
a (Å)	11.307(14)	9.810(12)	10.793(13)
b (Å)	10.427(13)	17.55(2)	14.456(16)
c (Å)	21.24(2)	14.214(17)	20.94(2)
β (°)	96.84(1)	97.60(1)	99.42(1)
V (Å^3)	2486	2425	3224(6)
Z	4	4	4
Calculated density (mg m^{-3})	1.959	2.180	1.813
Reflections measured	6799	7484	9883
Unique reflections/R_{int}	4039/0.0350	4441/0.0811	5539/0.0361
Data/restraints/parameters	4039/0/233	4441/0/236	5539/0/264
Final R indices [$I > 2\sigma(I)$]	$R_1 = 0.0410$, $wR_2 = 0.1098$	$R_1 = 0.0698$, $wR_2 = 0.1970$	$R_1 = 0.0737$, $wR_2 = 0.2068$
R indices (all data)	$R_1 = 0.0688$, $wR_2 = 0.1278$	$R_1 = 0.0906$, $wR_2 = 0.2112$	$R_1 = 0.1377$, $wR_2 = 0.2427$
Largest difference peak and hole (e Å^{-3})	1.345 and −1.747	2.583 and −2.356	2.961, −2.183

Table 6
Dimensions in the metal coordination sphere for the HC_2Bu^t complexes **5**–**7**

	5		**6**	**7**
W(1)–N(1)	2.167(10)	W(1)–C(11)	1.984(17)	2.004(16)
W(1)–C(100)	2.037(12)	W(1)–C(100)	2.030(17)	2.015(18)
W(1)–C(11)	2.072(12)	W(1)–C(12)	2.070(14)	2.037(14)
W(1)–C(12)	2.142(10)	W(1)–P(3)	2.472(4)	2.471(5)
W(1)–C(21)	2.067(11)	W(1)–P(2)	2.503(4)	2.504(5)
W(1)–C(22)	2.096(10)	W(1)–I(3)	2.827(3)	2.814(3)
W(1)–I(2)	2.883(3)	W(1)–I(2)	2.852(3)	2.851(3)
W(1)–I(3)	2.897(3)			
C(100)–W(1)–C(21)	74.2(4)	C(1)–W(1)–C(100)	115.3(6)	114.1(6)
C(100)–W(1)–C(11)	115.1(4)	C(11)–W(1)–C(12)	37.1(6)	36.2(6)
C(21)–W(1)–C(11)	104.0(4)	C(100)–W(1)–C(12)	78.4(7)	77.9(6)
C(100)–W(1)–C(22)	108.9(4)	C(11)–W(1)–P(3)	90.8(4)	89.1(4)
C(21)–W(1)–C(22)	35.1(4)	C(100)–W(1)–P(3)	88.9(5)	90.1(5)
C(11)–W(1)–C(22)	94.4(4)	C(12)–W(1)–P(3)	92.8(4)	91.5(4)
C(100)–W(1)–C(12)	80.6(4)	C(11)–W(1)–P(2)	77.7(5)	77.2(4)
C(21)–W(1)–C(12)	93.1(4)	C(100)–W(1)–P(2)	167.0(5)	168.7(5)
C(11)–W(1)–C(12)	34.6(4)	C(12)–W(1)–P(2)	114.7(5)	113.2(5)
C(22)–W(1)–C(12)	104.3(4)	P(3)–W(1)–P(2)	90.2(1)	91.8(4)
C(100)–W(1)–N(1)	157.6(4)	C(11)–W(1)–I(3)	101.8(4)	101.9(4)
C(21)–W(1)–N(1)	120.6(4)	C(100)–W(1)–I(3)	90.9(4)	89.0(5)
C(11)–W(1)–N(1)	79.4(4)	C(12)–W(1)–I(3)	100.8(4)	99.7(4)
C(22)–W(1)–N(1)	85.8(4)	P(3)–W(1)–I(3)	166.1(1)	168.3(1)
C(12)–W(1)–N(1)	112.9(4)	P(2)–W(1)–I(3)	86.9(1)	86.8(1)
C(100)–W(1)–I(2)	81.3(3)	C(11)–W(1)–I(2)	162.7(4)	163.9(4)
C(21)–W(1)–I(2)	88.7(3)	C(100)–W(1)–I(2)	78.7(5)	78.9(4)
C(11)–W(1)–I(2)	161.2(3)	C(12)–W(1)–I(2)	155.6(5)	155.6(4)
C(22)–W(1)–I(2)	88.2(3)	P(3)–W(1)–I(2)	78.8(1)	80.9(1)
C(12)–W(1)–I(2)	160.6(3)	P(2)–W(1)–I(2)	88.4(1)	90.4(1)
N(1)–W(1)–I(2)	82.3(3)	I(3)–W(1)–I(2)	87.5(1)	87.5(1)
C(100)–W(1)–I(3)	81.1(3)			
C(21)–W(1)–I(3)	154.8(3)			
C(11)–W(1)–I(3)	91.0(3)			
C(22)–W(1)–I(3)	165.2(3)			
C(12)–W(1)–I(3)	88.0(3)			
N(1)–W(1)–I(3)	81.6(3)			
I(2)–W(1)–I(3)	82.34(5)			

$[WI_2(CO)(NCR)(\eta^2\text{-}MeC_2Ph)_2]$ [21], [2.012(10) Å (R = Me) and 2.043(15) Å, (R = Et)]. The alkyne carbon–tungsten bond lengths for $[WI_2(CO)(NCPh)(\eta^2\text{-}MeC_2Ph)_2]$ [21], [2.040(2) Å, 2.117(5) Å-Me; 2.145(17) Å, 2.110(18) Å-Ph] and **5** [2.067(11) Å, 2.072(12) Å-H; 2.142(10) Å, 2.096(10) Å-Bu^t] are all similar, with the W–C(R) bond (for R = Me, H) being shorter than the W–C(R′) bond (for R = Ph, Bu^t), which can be explained in terms of the electron withdrawing/donating properties of the different substituents.

In the four complexes $[WI_2(CO)(NCR)(\eta^2\text{-}MeC_2Ph)_2]$ (R = Me, Et, Ph) [21] and **5**, the average back bend angle, β, was calculated from the R–C–C and R′–C–C angles with $[WI_2(CO)(NCMe)(\eta^2\text{-}MeC_2Ph)_2]$ at 36.5° (Me) and 34.2° (Ph) [21], $[WI_2(CO)(NCEt)(\eta^2\text{-}MeC_2Ph)_2]$ at 35.8° (Me) and 37.0° (Ph) [21], $[WI_2(CO)(NCPh)(\eta^2\text{-}MeC_2Ph)_2]$ at 36.4° (Me), 41.0° (Me), 32.9° (Ph) and 34.8° (Ph) [21], and **5** at 37.0° (Bu^t) and 36.7° (Bu^t), with all β-angles in the region of 30–40°, as expected [23].

2.3. Preparation and characterisation of $[WI_2(CO)\{P(OR)_3\}_2(\eta^2\text{-}HC_2Bu^t)]$ *(R = Me, Et, Pr^i) (**6**–**8**)*

Reaction of $[WI_2(CO)(NCMe)(\eta^2\text{-}HC_2Bu^t)_2]$ **1** with two equivalents of $P(OR)_3$ (R = Me, Et or Pr^i) in Et_2O at room temperature gave the deep green bis(phosphite) complexes, $[WI_2(CO)\{P(OR)_3\}_2(\eta^2\text{-}HC_2Bu^t)]$ **6**–**8**, in excellent yield. Complexes **6**–**8** have been fully characterised by elemental analysis (C, H and N) (Table 1), IR spectroscopy (Table 2), ^1H and $^{31}P\{^1H\}$-NMR spectroscopy (Tables 3 and 7). Complexes **6** and **7** were also characterised by de-coupled $^{13}C\{^1H\}$ and by coupled ^{13}C–^1H-NMR spectroscopy, and their molecular structures determined by X-ray crystallography. All three bis(phosphite) complexes were very soluble in

Table 7
Boron and phosphorus NMR data [a,b] for the HC_2Bu^t complexes **6**–**11**

	$^{11}B\{^1H\}$ (δ) [a] ppm	$^{31}P\{^1H\}$ (δ) ppm [b]
6		114.67 (d, 1P, $J_{P-P} = 28.2$ Hz, $J_{W-P} = 143.4$ Hz)-*cis*; 102.79 (d, 1P, $J_{P-P} = 28.2$ Hz, $J_{W-P} = 254.5$ Hz)-*cis*
7		113.28 (d, 1P, $J_{P-P} = 29.8$ Hz, $J_{W-P} = 139.8$ Hz)-*cis*; 97.47 (d, 1P, $J_{P-P} = 29.8$ Hz, $J_{W-P} = 255.9$ Hz)-*cis*
8		107.29 (d, 1P, $J_{P-P} = 29.5$ Hz, $J_{W-P} = 105.8$ Hz)-*cis*; 94.04 (d, 1P, $J_{P-P} = 29.5$ Hz)-*cis*; 92.27 (s, 2P, $J_{W-P} = 214.6$ Hz)-*trans*
9	−1.41, s	108.84 (s, $J_{W-P} = 220.5$ Hz)-*trans*
10	−1.41, s	103.90 (s, $J_{W-P} = 219.7$ Hz)-*trans*
11	−1.41, s	100.76 (s)-*trans*

s, Singlet; d, doublet; t, triplet; m, multiplet.

[a] Spectra recorded in $CDCl_3$ at +25 °C, referenced to $BF_3 \cdot OEt_2$.

[b] Spectra recorded in $CDCl_3$ at +25 °C, referenced to 85% H_3PO_4.

CH_2Cl_2, $CHCl_3$ and Et_2O, but were insoluble in hydrocarbon solvents. Complexes **6**–**8** were moderately air-stable and could be handled in air for short periods. When solutions are exposed to air, the complexes decompose within 24 h. The complexes can all be stored under nitrogen at −17 °C for up to 1 month, but solutions will decompose after 1 month even under a nitrogen atmosphere at −17 °C.

Suitable single crystals of $[WI_2(CO)\{P(OR)_3\}_2(\eta^2\text{-}HC_2Bu^t)]$ {R = Me (**6**) and Et (**7**)}for a single crystal X-ray diffraction study were grown by cooling concentrated diethyl ether solutions of **6** and **7** to −17 °C for 24 h, and their structures are shown in Figs. 3 and 4, respectively. Crystal data and structural refinement for both **6** and **7** are given in Table 5, and dimensions in the metal coordination spheres are given in Table 6. The structures of **6** and **7** are very similar, as detailed by their dimensions in Table 6, and their structures in Figs. 3 and 4. For both complexes, the two phosphite ligands are shown to be mutually *cis*. In previous work [24,25], we have shown that compounds of general formula, $[MI_2(CO)\{P(OR)_3\}_2(\eta^2\text{-}RC_2R)]$ are predominately *trans*, with respect to the phosphite ligands, although two examples of *cis* structures have been structurally characterised, namely $[MI_2(CO)\{P(OMe)_3\}_2(\eta^2\text{-}MeC_2Me)]$ (M = Mo [25], W [24]). The geometry of these isomorphous compounds is similar to that found in **6** and **7**, the M–P bond *trans* to the carbonyl is longer than that *trans* to the iodine [M = Mo, 2.516(3), 2.469 Å; M = W, 2.502(6), 2.451(6) Å] [24,25] which is also observed for **6** [2.503(4), 2.472(4) Å] and **7** [2.504(2), 2.471(5) Å]. In all four complexes, it is also apparent that the iodine *trans* to the phosphite forms a slightly shorter bond to the metal than the iodine *trans* to the alkyne ligand.

The impetus for the formation of the *trans* form of these compounds may well be crystal packing, as in two of the examples characterised, namely $[MI_2(CO)\{P(OPr^i)_3\}_2(\eta^2\text{-}MeC_2Me)]$ (M = Mo, W) [25], the *trans* molecules contain crystallographic C_2 symmetry with disorder between the carbonyl and 2-butyne. In an

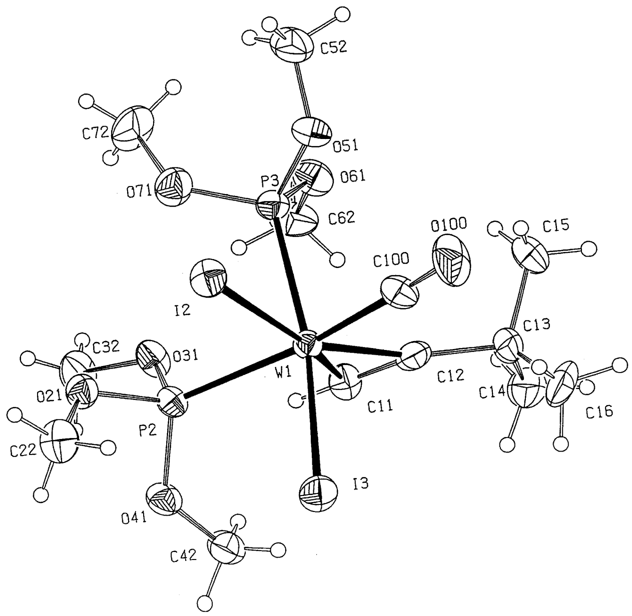

Fig. 3. Crystal structure of $[WI_2(CO)\{P(OMe)_3\}_2(\eta^2\text{-}HC_2Bu^t)]$ **6**, together with the atomic numbering scheme; ellipsoids shown at 30% probability.

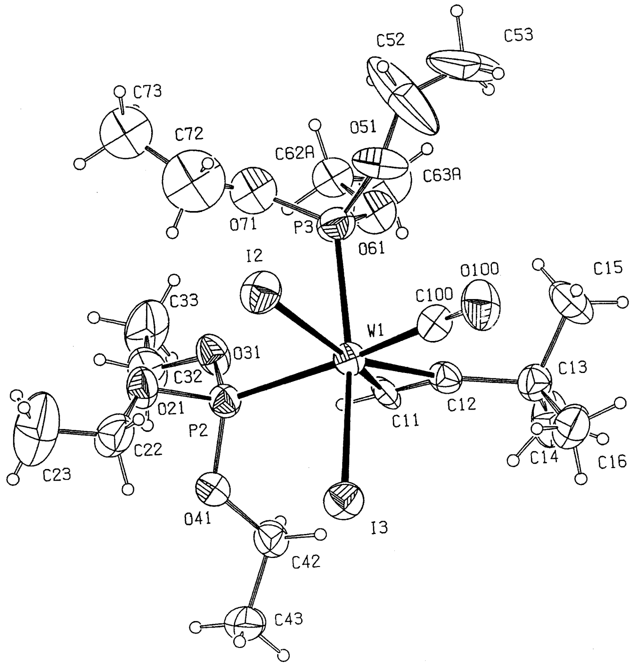

Fig. 4. Crystal structure of $[WI_2(CO)\{P(OEt)_3\}_2(\eta^2\text{-}HC_2Bu^t)]$ **7**, together with the atomic numbering scheme; ellipsoids shown at 20% probability.

additional case, $[WI_2(CO)\{P(OEt)_3\}_2(\eta^2\text{-}MeC_2Me)]$ [25], this disorder is present, even without the crystallographic symmetry. However, in the present examples, it seems likely that the asymmetry of the alkyne, and indeed the bulk of the *tert*-butyl substituent, prevents the disorder and leads to the stabilisation of the *cis* form, where the bulky *tert*-butyl group of the alkyne is directed away from both phosphite ligands.

The IR spectra of **6**–**8** have strong, broad carbonyl stretching bands at 1999, 1992 and 1981 cm^{-1}, respectively. The solid state structures of **6** and **7** have *cis*-phosphites, with the carbonyl ligand *trans* to a π-accepting phosphite group. The NMR spectroscopic data for **6** and **7** supports an exclusively *cis*-phosphite geometry in solution (see later in this section). However, complex **8**, $[WI_2(CO)\{P(OPr^i)_3\}_2(\eta^2\text{-}HC_2Bu^t)]$, exists as a mixture of *cis*- and *trans*-phosphite isomers in solution (Fig. 5), which is also supported by NMR studies. Therefore, the *trans*-isomer of **8** has the carbonyl *trans* to an iodo-group which is not a π-acceptor, and, therefore, results in a lower carbonyl stretching band than those of **6** and **7**. The alkyne stretching bands (Table 2) are at lower wavenumbers than those for the uncoordinated alkyne, due to synergic bonding.

The ^1H-NMR spectra (Table 3) of **6**–**8** confirm that **6** and **7** exist only as the *cis*-isomers in solution, whereas complex **8** forms a mixture of *cis*:*trans* isomers with an approximate integral ratio of 40:60. These results are very different to those previously observed for the related 2-butyne, 1-phenyl-1-propyne and diphenylacetylene complexes, $[WI_2(CO)\{P(OR)_3\}_2(\eta^2\text{-}R'C_2R'')]$ [24,25], which generally have mixtures of *cis* and *trans* isomers in solution. The greatest proportion of *cis*-isomer is associated with the smallest phosphite, $P(OMe)_3$, cone angle 107° [26], whilst the bulkiest phosphite, $P(OPr^i)_3$, cone angle 130° [26], results in exclusive formation of the *trans*-isomer for these three alkynes, in solution and in the solid state [25]. However, for the 3,3-dimethyl-1-butyne complexes described here, there is competition from the very large *tert*-butyl substituent on the alkyne and the large triisopropylphosphite ligands, which results in *cis*- and *trans*-isomers of **8** being formed.

The sole formation of the *cis*-isomer of **6** and **7** (Figs. 3 and 4), shows that for small cone angle phosphites [26], the size of the *tert*-butyl group is sufficient to prevent *trans*-isomer formation. It may be that the bulky *tert*-butyl substituent hinders a trigonal twist mechanism, which probably occurs after the initial formation of the *cis*-isomer, thus affording the crowded *cis*-complex only (Scheme 1). For the largest cone angle phosphite complex, **8**, some rearrangement occurs in solution, giving the only example of a bis(triisopropylphosphite) complex of this type which forms both the *cis*- and *trans*-isomers in solution. The proposed mechanism for the formation of **6**–**8** is given in Scheme 1.

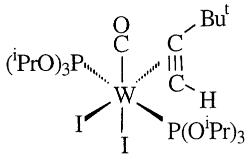

Fig. 5. Proposed structure of *trans*-$[WI_2(CO)\{P(OPr^i)_3\}_2(\eta^2\text{-}HC_2Bu^t)]$ **8**.

As complexes **6** and **7** exist as single isomers in solution, proton coupled ^{13}C-NMR spectroscopy has been used to distinguish between the two alkyne contact carbon resonances on the unsymmetric terminal alkyne ligand. In the proton-coupled carbon NMR spectrum of **6**, the high-field resonance at 190.95 ppm [dd, $J_{C-C} = 8.7$ Hz, $J_{P-C} = 35.8$ Hz] is further split into a double doublet of doublets and so was assigned to $H\mathbf{C}{\equiv}CBu^t$, [ddd $J_{C-C} = 8.4$ Hz, $J_{P-C} = 36.0$ Hz, $J_{C-H} = 210.7$ Hz]. This alkyne carbon–hydrogen coupling value compares with those determined by Templeton et al. [27], for similar molybdenum complexes, $[MoBr_2(CO)(PEt_3)_2(\eta^2\text{-}HC_2Ph)]$ (alkyne $J_{C-H} = 204$ Hz) and $[MoBr_2(CO)(dppe)(\eta^2\text{-}HC_2^nBu)]$ (alkyne $J_{C-H} = 215$ Hz). The signal at 213.12 ppm, [dd, $J_{C-C} = 8.7$ Hz, $J_{P-C} = 66.6$ Hz], remained unchanged and was assigned to the *tert*-butyl substituted carbon of 3,3-dimethyl-1-butyne. The same pattern was observed for the ^{13}C–^1H-NMR spectrum of complex **7**, giving an alkyne carbon–hydrogen coupling of $J_{C-H} = 210.2$ Hz, which supported the peak assignments. Fig. 6 shows the regions 230–180 ppm for both the $^{13}C\{^1H\}$-NMR spectrum (a) and ^{13}C–^1H-NMR spectrum (b) of complex **6**. The resonances above 200 ppm for the alkyne contact carbons suggest [20] that the 3,3-dimethyl-1-butyne ligand is donating four electrons to the tungsten in both **6** and **7**, which also enables them to obey the effective atomic number rule.

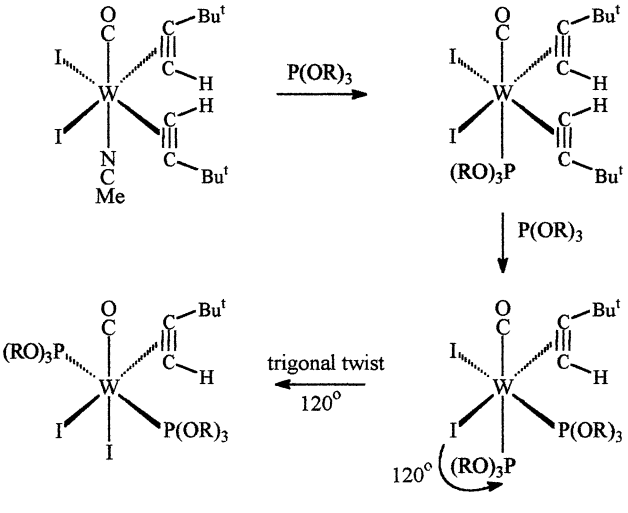

Scheme 1. Proposed mechanism for the reaction of $[WI_2(CO)(NCMe)(\eta^2\text{-}HC_2Bu^t)_2]$ **1** with $P(OR)_3$, to afford complexes **6**–**8**.

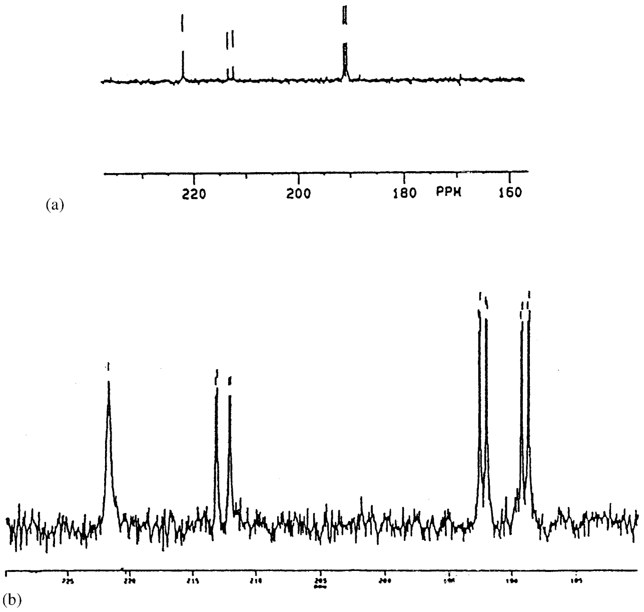

Fig. 6. The alkyne (C≡C) contact carbon region for (a) the $^{13}C\{^1H\}$-NMR spectrum and (b) the $^{13}C-^1H$-NMR spectrum of *cis*-$[WI_2(CO)\{P(OMe)_3\}_2(\eta^2\text{-}HC_2Bu^t)]$ **6**, ($CDCl_3$, 25 °C, referenced to $SiMe_4$).

The $^{31}P\{^1H\}$-NMR spectra (Table 7) show, as expected, two doublets for the *cis*-isomers of $[WI_2(CO)\{P(OR)_3\}_2(\eta^2\text{-}HC_2Bu^t)]$ {R = Me **6** and Et **7**} and a mixture of two doublets (*cis*-isomer) and one singlet (*trans*-isomer) for the bis(triisopropylphosphite) analogue, $[WI_2(CO)\{P(OPr^i)_3\}_2(\eta^2\text{-}HC_2Bu^t)]$ **8**, in a similar ratio to that observed in the proton NMR spectrum of **8**.

2.4. Preparation and characterisation of $[WI(CO)(NCMe)\{P(OR)_3\}_2(\eta^2\text{-}HC_2Bu^t)][BF_4]$ (R = Me, Et, Pr^i) (9–11)

Equimolar quantities of $[WI_2(CO)\{P(OR)_3\}_2(\eta^2\text{-}HC_2Bu^t)]$ (**6**–**8**) and $Ag[BF_4]$ react in acetonitrile at room temperature, and in the absence of light, to give the new cationic complexes, $[WI(CO)(NCMe)\{P(OR)_3\}_2(\eta^2\text{-}HC_2Bu^t)][BF_4]$ {R = Me (**9**); Et (**10**); Pr^i (**11**)}, as red–brown oils and in good yield. The complexes were fully characterised by elemental analysis (C, H and N) (Table 1), IR spectroscopy (Table 2), ^1H-NMR spectroscopy (Table 3) and ^{11}B and ^{31}P-NMR (Table 7). The complexes are all highly soluble in NCMe, CH_2Cl_2 and acetone, but as expected, are insoluble in diethyl ether and hydrocarbon solvents due to their ionic nature.

The IR spectra of **9**–**11** show carbonyl bands at $\nu(CO) = 1985$, 1978 and 1976 cm^{-1}, respectively, and weak nitrile stretching bands at ca. 2300 cm^{-1}. The ^1H-NMR spectra (Table 3) all showed singlet resonances due to the terminal alkyne protons at $\delta = 13.95$, 13.70 and 13.55 ppm, respectively, which suggests the formation of a single isomer in solution. The low-field positions of the terminal alkyne proton resonances for complexes **9**–**11** indicate that the 3,3-dimethyl-1-butyne ligand is acting as a four electron donor [18,19] to the tungsten centre.

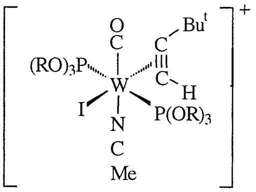

Fig. 7. Proposed structure of the cations, $[WI(CO)(NCMe)\{P(OR)_3\}_2(\eta^2\text{-}HC_2Bu^t)]^+$ (**9**–**11**).

The $^{31}P\{^1H\}$-NMR spectra (Table 7) of complexes **9**–**11** showed singlet resonances at $\delta = 108.84$ ($J_{W-P} = 220.5$ Hz), 103.90 ($J_{W-P} = 219.7$ Hz) and 100.76 ppm, which indicates the exclusive formation of the *trans*-isomer. The ^{11}B-NMR spectra of complexes **9**–**11** all show a single resonance at $\delta = -1.41$ ppm due to the tetrafluoroborate anion, $[BF_4]^-$, which confirms the ionic nature of the complexes.

It is interesting to note that whilst the cationic complexes **9**–**11** are obtained as the *trans*-phosphite isomer, exclusively, the neutral precursors, $[WI_2(CO)\{P(OR)_3\}_2(\eta^2\text{-}HC_2Bu^t)]$ {**6** (R = Me); **7** (R = Et)}, exist only as the *cis*-phosphite isomer in both the solid state (Figs. 3 and 4) and in solution (Tables 3, 4 and 7). After displacement of one iodide by an acetonitrile ligand during the reaction of $[WI_2(CO)\{P(OR_3\}_2(\eta^2\text{-}H_2Bu^t)]$ {**6** (R = Me); **7** (R = Et); **8** (R = Pr^i)} with $Ag[BF_4]$ in acetonitrile, the neutral complexes **6**–**8** undergo a *cis* to *trans* isomerism, probably via a trigonal twist mechanism, as described earlier for the formation of the *trans* isomer of complex **8**. An alternative mechanism, which cannot be discounted, might be the initial removal of the iodide to give a five co-ordinate species which could rearrange more readily than a six co-ordinate complex. The proposed structures of the cationic complexes **9**–**11** (Fig. 7) are based upon the structure of the related 2-butyne complex, $[WI(CO)(NCMe)\{P(OPr^i)_3\}_2(\eta^2\text{-}MeC_2Me)][BPh_4]$, which has been previously reported [28].

3. Conclusions

We have observed that the reaction of an unsymmetrical alkyne with our $[WI_2(CO)_3(NCMe)_2]$ system [2,29], affords different stereochemical products which was not observed for our symmetrical alkyne work with, for example, 2-butyne and diphenylacetylene. An interesting *cis*- to *trans*-phosphite isomerism occurs when an iodide ligand is removed from $[WI_2(CO)\{P(OR)_3\}_2(\eta^2\text{-}$

HC_2Bu^t)] {**6** (R = Me); **7** (R = Et); **8** (R = Pr^i)} using Ag[BF_4] in acetonitrile to give the cationic complexes, [WI(CO)(NCMe){$P(OR)_3$}$_2$(η^2-HC_2Bu^t)] {**9** (R = Me); **10** (R = Et); **11** (R = Pr^i)}. We are currently exploring the reactions of other highly unsymmetrical alkynes with our [$MI_2(CO)_3(NCMe)_2$] systems.

4. Experimental

4.1. General remarks

The preparation and purification of complexes **1**–**11** prepared in this paper were carried out under an atmosphere of dry nitrogen using standard vacuum/Schlenk-line techniques. The starting material, [$WI_2(CO)_3(NCMe)_2$], was prepared by the literature method [16,30]. All other chemicals used were purchased from commercial sources. All solvents were dried before use.

Elemental analyses (C, H and N) were recorded on a Carlo Erba Elemental Analyser MOD 1106, (using helium as a carrier gas). Infra-red spectra were recorded on a Perkin–Elmer 1600 series FTIR spectrophotometer, as thin films in chloroform ($CHCl_3$). All NMR spectra were recorded on a Bruker AC 250 CP–MAS NMR spectrometer, with ^1H, ^{13}C-NMR and $^{13}C\{^1H\}$-NMR spectra referenced to $SiMe_4$, ^{11}B-NMR Spectra referenced to $BF_3 \cdot OEt_2$ and $^{31}P\{^1H\}$-NMR referenced to 85% H_3PO_4.

4.2. Synthesis of [$WI_2(CO)(NCMe)(\eta^2$-$HC_2Bu^t)_2$] (1)

To a solution of [$WI_2(CO)_3(NCMe)_2$] (4.542 g, 7.522 mmol) in CH_2Cl_2 (35 cm^3), in a foil-covered Schlenk tube, 3,3-dimethyl-1-butyne (1.852 ml, 1.236 g, 15.045 mmol) was added and the solution stirred for 22 h. The resultant gold-brown solution was filtered over celite, followed by removal of the solvent in vacuo, gave the product, [$WI_2(CO)(NCMe)(\eta^2$-$HC_2Bu^t)_2$], **1**, as a gold–yellow solid, yield = 4.436 g, 88%. For physical and analytical data, refer to Table 1.

4.3. Synthesis of [$WI_2(CO)(NCPh)(\eta^2$-$HC_2Bu^t)_2$] (5)

To a solution of [$WI_2(CO)(NCMe)(\eta^2$-$HC_2Bu^t)_2$] (0.505 g, 0.753 mmol) in dichloromethane (30 cm^3), benzonitrile (PhCN) (0.077 ml, 0.078 g, 0.753 mmol) was added and the solution stirred for 22 h. The resultant gold–green solution was filtered over celite and the solvent volume reduced in vacuo, to ~5 cm^3. Recrystallisation from dichloromethane–diethyl ether solution (5:6 cm^3), cooled to −17 °C, gave single green–yellow crystals of the product, [WI_2(CO)(NCPh)(η^2-$HC_2Bu^t)_2$], **5**, yield = 0.403 g, 77%.

Similar reactions of equimolar quantities of [$WI_2(CO)(NCMe)(\eta^2$-$HC_2Bu^t)_2$] and NCR in CH_2Cl_2 at room temperature (r.t.) gave the acetonitrile exchanged products, [$WI_2(CO)(NCR)(\eta^2$-$HC_2Bu^t)_2$] {**2** (R = Me); **3** (R = Et); **4** (R = Pr^i)}. For physical and analytical data, refer to Table 1.

4.4. Synthesis of [$WI_2(CO)\{P(OEt)_3\}_2(\eta^2$-$HC_2Bu^t)$] (7)

To a solution of [$WI_2(CO)(NCMe)(\eta^2$-$HC_2Bu^t)_2$] (1.700 g, 2.533 mmol) in diethyl ether (25 cm^3), triethylphosphite, [$P(OEt)_3$], (0.878 cm^3, 0.842 g, 5.067 mmol) was added and the solution stirred for 45 min. The resultant solution was filtered over celite, the solvent reduced to minimum volume (5 cm^3) in vacuo and cooled to −17 °C for 18 h. Dark green single crystals of the product, [$WI_2(CO)\{P(OEt)_3\}_2(\eta^2$-$HC_2Bu^t)$] **7**, suitable for X-ray crystallography were obtained, yield = 2.010 g, 90%.

Using analogous methods, complexes **6**, [$WI_2(CO)$-{$P(OMe)_3$}$_2$(η^2-HC_2Bu^t)], and **8**, [$WI_2(CO)\{P(OPr^i)_3\}_2$-(η^2-HC_2Bu^t)], were prepared. Single crystals of **6** suitable for X-ray crystallography were grown from a concentrated Et_2O solution, cooled to −17 °C, for 24 h. For physical and analytical data, refer to Table 1.

4.5. Synthesis of [$WI(CO)(NCMe)\{P(OEt)_3\}_2(\eta^2$-$HC_2Bu^t)$][$BF_4$] (10)

To a solution of [$WI_2(CO)\{P(OEt)_3\}_2(\eta^2$-$HC_2Bu^t)$] (1.505 g, 1.710 mmol) in acetonitrile (30 cm^3), in a foil-covered Schlenk tube, silver tetrafluoroborate, Ag[BF_4], (0.333 g, 1.711 mmol) was added and the solution stirred for 22 h. The solvent was removed under vacuum and the crude product dissolved in CH_2Cl_2 (30 cm^3). The resultant deep red-brown solution was filtered over celite (×3) to remove all traces of the cream by-product, silver iodide. The solvent was reduced to minimum volume (5 cm^3) in vacuo and the concentrated solution washed with Et_2O (3 × 10 cm^3). The cationic product, [$WI(CO)(NCMe)\{P(OEt)_3\}_2(\eta^2$-$HC_2Bu^t)$]-[$BF_4$], **10**, was dried under vacuum for 24 h, to give a dark red–brown oil, yield = 0.995 g, 63%.

The cationic complexes [WI(CO)(NCMe)-{$P(OMe)_3$}$_2$(η^2-HC_2Bu^t)][BF_4], **9** and [WI(CO)(NCMe){$P(OPr^i)_3$}$_2$(η^2-HC_2Bu^t)][BF_4], **11** were prepared by analogous methods, and despite repeated recrystallisation, could only be obtained as oils. For physical and analytical data, refer to Table 1.

4.6. X-ray crystallographic study

Crystal data for **5**–**7** are given in Table 5, together with refinement details. The structures of **5**–**7** were determined by single crystal X-ray diffraction techniques. Cell data and refinement details are given in Table 5. Crystal data were collected with Mo–K_{α} radiation using the MARresearch Image Plate System. The crystals were positioned at 70 mm from the Image Plate. 100 frames were measured at 2° intervals with a counting time of 2 min. Data analysis was carried out with the XDS program [31]. The structures were solved using direct methods with the SHELX 86 program [32]. In **7**, one ethyl group was disordered over two positions and the alternatives were refined with 50% occupancy.

In all three structures, the non-hydrogen atoms were refined with anisotropic thermal parameters apart from the disordered atoms. The hydrogen atoms were included in geometric positions and given thermal parameters equivalent to 1.2 times those of the atom to which they were attached. Empirical absorption corrections were carried out using the DIFABS program [33]. The structures were refined on F^2 using SHELXL [34].

5. Supplementary material

Crystallographic data (excluding structure factors) for the structures reported in this paper have been deposited at the Cambridge Crystallographic Data Centre as supplementary publication number CCDC-163087 (**5**), CCDC-163088 (**6**) and CCDC-163089 (**7**). Copies of the data can be obtained free of charge from The Director, CCDC, 12 Union Road, Cambridge CB2 1EZ, UK (Fax: +44-1223-336033; e-mail: deposit@ccdc.cam.ac.uk or www: http://www.ccdc.cam.ac.uk).

Acknowledgements

D.S.M. thanks the EPSRC for a Research Studentship. We also thank the EPSRC and the University of Reading for funds for the image plate system. We also thank A.W. Johans for help with the crystallographic work.

References

[1] J.L. Templeton, Adv. Organomet. Chem. 29 (1989) 1 (and references cited therein).

[2] P.K. Baker, Adv. Organomet. Chem. 40 (1996) 45 (and references cited therein).

[3] N.G. Aimeloglou, P.K. Baker, M.M. Meehan, M.G.B. Drew, Polyhedron 17 (1998) 3455.

[4] M. Bottrill, M. Green, J. Chem. Soc. Dalton Trans. (1977) 2365.

[5] S.R. Allen, P.K. Baker, S.G. Barnes, M. Green, L. Trollope, L. Manojlović-Muir, K.W. Muir, J. Chem. Soc. Dalton Trans. (1981) 873.

[6] J.L. Davidson, D.W.A. Sharp, J. Chem. Soc. Dalton Trans. (1975) 2531.

[7] J.L. Davidson, G. Vasapollo, J. Chem. Soc. Dalton Trans. (1985) 2239.

[8] E.M. Armstrong, P.K. Baker, M.G.B. Drew, Organometallics 7 (1988) 319.

[9] J.L. Davidson, G. Vasapollo, J. Chem. Soc. Dalton Trans. (1988) 2855.

[10] P.K. Baker, A. Bury, K.R. Flower, Polyhedron 8 (1989) 2587.

[11] (a) E.M. Armstrong, P.K. Baker, S.G. Fraser, J. Chem. Res. (S) (1988) 52;
(b) E.M. Armstrong, P.K. Baker, S.G. Fraser, J. Chem. Res. (M) (1988) 0410.

[12] J.L. Davidson, J. Organomet. Chem. 419 (1991) 137.

[13] J.L. Davidson, G. Vasapollo, J.C. Millar, K.W. Muir, J. Chem. Soc. Dalton Trans. (1987) 2165.

[14] M. Al-Jahdali, P.K. Baker, M.G.B. Drew, Z. Naturforsch. Sect. B 54 (1999) 171.

[15] J.L. Davidson, G. Vasapollo, Polyhedron 2 (1983) 305.

[16] P.K. Baker, S.G. Fraser, E.M. Keys, J. Organomet. Chem. 309 (1986) 319.

[17] R.M. Silverstein, G.C. Bassler, T.C. Morrill, Spectroscopic Identification of Organic Compounds, 5th ed., Wiley-Interscience, Wiley, Chichester, 1991.

[18] M. Kamata, K. Hirotsu, T. Higuchi, M. Kido, K. Tatsumi, T. Yoshida, S. Otsuka, Inorg. Chem. 22 (1983) 2416.

[19] B.C. Ward, J.L. Templeton, J. Am. Chem. Soc. 102 (1980) 1532.

[20] J.L. Templeton, B.C. Ward, J. Am. Chem. Soc. 102 (1980) 3288.

[21] P.K. Baker, M.G.B. Drew, D.S. Evans, Can. J. Chem. 79 (2001) 263.

[22] M.G.B. Drew, P.K. Baker, D.J. Muldoon, A.J. Lavery, A. Shawcross, Gazz. Chim. Ital. 126 (1996) 625.

[23] M. Bochmann, Organometallics 2-Complexes with Transition Metal–Carbon π-bonds, (1996 reprint), Oxford Science Publications, Oxford University Press, Oxford.

[24] P.K. Baker, E.M. Armstrong, M.G.B. Drew, Inorg. Chem. 28 (1989) 2406.

[25] P.K. Baker, M.G.B. Drew, D.S. Evans, A.W. Johans, M.M. Meehan, J. Chem. Soc. Dalton Trans. (1999) 2541.

[26] C.A. Tolman, Chem. Rev. 77 (1977) 313.

[27] P.B. Winston, S.J.N. Burgmayer, T.L. Tonker, J.L. Templeton, Organometallics 5 (1986) 1707.

[28] P.K. Baker, D.S. Evans, M.G.B. Drew, Inorg. Chem. Commun. 2 (1999) 169.

[29] P.K. Baker, Chem. Soc. Rev. 27 (1998) 125 (and references cited therein).

[30] P.K. Baker, M.M. Meehan, Inorg. Synth. 33 (2002) 239.

[31] W. Kabsch, J. Appl. Crystallogr. 21 (1988) 916.

[32] SHELXS 86, G.M. Sheldrick, Acta Crystallogr. Sect. A 46 (1990) 467.

[33] N. Walker, D. Stuart, Acta Crystallogr. Sect. A 39 (1983) 158.

[34] G.M. Sheldrick, SHELXL Program for Crystal Structure Refinement, University of Göttingen, 1993.